Out-of-plane polarization in a layered manganese chloride hybrid

Kamminga, Machteld; Hidayat, Romel; Baas, Jacobus; Blake, Graeme; Palstra, Thomas

Published in:
APL Materials

DOI:
10.1063/1.5024857

Out-of-plane polarization in a layered manganese chloride hybrid

Machteld E. Kamminga, Romel Hidayat, Jacob Baas, Graeme R. Blake, and Thomas T. M. Palstra

Citation: APL Materials **6**, 066106 (2018); doi: 10.1063/1.5024857
View online: https://doi.org/10.1063/1.5024857
View Table of Contents: http://aip.scitation.org/toc/apm/6/6
Published by the American Institute of Physics

APL MATERIALS **6**, 066106 (2018)

Out-of-plane polarization in a layered manganese chloride hybrid

Machteld E. Kamminga,[1] Romel Hidayat,[1,2] Jacob Baas,[1] Graeme R. Blake,[1] and Thomas T. M. Palstra[1,a]

[1]*Zernike Institute for Advanced Materials, University of Groningen, Nijenborgh 4, 9747 AG Groningen, The Netherlands*

[2]*Faculty of Mathematics and Natural Sciences, Institut Teknologi Bandung, Jl. Ganesha 10, Bandung 40132, Indonesia*

(Received 5 February 2018; accepted 5 April 2018; published online 13 June 2018)

We investigate possible mechanisms to induce electric polarization in layered organic-inorganic hybrids. Specifically, we investigate the structural phase transitions of PEA_2MnCl_4 (PEA = phenethylamine) using temperature dependent single-crystal X-ray diffraction analysis, including the symmetry analysis of the observed space groups. Our results show that PEA_2MnCl_4 transforms from a high-temperature centrosymmetric structure with space group $I4/mmm$ to a low-temperature polar $Pca2_1$ phase via an intermediate phase with polar space group $Aea2$. We study the mechanism responsible for the $I4/mmm$ to $Aea2$ polar phase transition and find that it is different from previously proposed mechanisms in similar systems. The transition is governed by the opening of a small dihedral angle between the phenyl ring planes of two adjacent PEA molecules, which consequently become crystallographically inequivalent in the $Aea2$ phase. This molecular rotation induces a significant difference in the lengths of the ethylammonium tails of the two molecules, which coordinate the inorganic layer asymmetrically and are consequently involved in different hydrogen bonding patterns. Consequently, the negatively charged chlorine octahedron that coordinates the Mn^{2+} cation deforms. This deformation moves the Mn^{2+} off-center along the out-of-plane-axis, contributing to the polar nature of the structure. Notably, the polar axis is out-of-plane with respect to the inorganic sheets. This is in contrast to other layered organic-inorganic hybrids as well as conventional layered perovskites, such as the Aurivillius phases, where in-plane polarization is observed. Our findings add to the understanding of possible mechanisms that can induce ferroelectric behavior in layered organic-inorganic hybrids. https://doi.org/10.1063/1.5024857

Organic-inorganic hybrid materials are of great interest for a wide range of applications. The combination of organic and inorganic components in a single compound leads to a class of materials that exhibits a large variety of properties including the two-dimensional magnetic order[1,2] and the coexistence of ferromagnetic and ferroelectric ordering.[3,4] Recently, organic-inorganic hybrids have also attracted growing attention for optoelectronic applications such as light-emitting diodes,[5,6] lasers,[7,8] photodetectors,[9] and efficient planar heterojunction solar cell devices.[10–14]

Organic-inorganic hybrids can adopt the perovskite structure ABX_3; a variety of organic cations can occupy the 12-fold coordinated A-sites, which are enclosed by metal halide BX_6-octahedra. When organic cations that are too large for this coordination geometry are introduced, layered structures with structural formula A_2BX_4 can be obtained. These layered hybrids consist of single ⟨100⟩-terminated perovskite sheets separated by bilayers of the organic cations and are held together by van der Waals interactions between the organic groups.[15] Such materials can benefit from enhanced conduction

[a]Present address: University of Twente, Enschede, The Netherlands. E-mail: t.t.m.palstra@rug.nl

within the layers[15] and have potential applications in field-effect transistors and light emission.[5,6] Furthermore, these layered structures tend to be more stable against humidity.[16]

Similar to oxide perovskites, hybrids can exhibit ferroelectric and piezoelectric properties at room temperature.[3,17–21] Polar hybrids are of interest for various applications, which depend on the crystallographic polar axis. For example, it is thought that solar cells can benefit from a ferroelectric domain structure, as charge separation is a key aspect of their performance.[22,23] A built-in electric field can assist exciton separation and charge transport. In layered structures, this requires that the polar axis lies in-plane with respect to the layers. On the other hand, ferroelectric-gate field-effect transistors (FeFETs) require charge induction and can benefit from a polar material as the gate electrode: the top electrode can change the resistance by changing the polarization.[24] This application requires a polar axis that lies out-of-plane. The buckling of the inorganic layers that usually occurs in layered hybrid perovskites can result in a rotational degree of freedom of the octahedra that gives rise to in-plane polarization.[25] We have previously observed such a mechanism in the layered phenethylammonium (PEA) copper-chloride hybrids PEA_2CuCl_4,[3] where the polar-to-non-polar phase transition at 430 K is associated with the onset of the buckling of the inorganic lattice.

In this work, we focus on structural phase transitions in the layered PEA manganese chloride hybrid. PEA_2MnCl_4 and PEA_2CuCl_4 contain the same PEA organic moiety and have similar structural features, and we find that they both have two structural phase transitions at similar temperatures (363 K and 412 K for the former and 340 K and 410 K for the latter). The major difference is that the Cu^{2+} cation in PEA_2CuCl_4 is Jahn-Teller (JT) active, whereas Mn^{2+} in PEA_2MnCl_4 is not. Therefore, PEA_2CuCl_4 has a significantly distorted inorganic lattice involving an alternating pattern of long and short Cu—Cl bonds in plane; the $MnCl_6$-octahedra in PEA_2MnCl_4 are much more regular. The spatially ordered configuration of magnetic orbitals associated with this bonding pattern in PEA_2CuCl_4 gives rise to the ferromagnetic order below 13 K,[3,26] whereas the (canted) antiferromagnetic order is observed below 44.3 K in PEA_2MnCl_4.[27,28] The presence or absence of a JT-active cation also has a major influence on the buckling of the inorganic lattice and the corresponding buckled-to-non-buckled phase transition. In contrast to PEA_2CuCl_4,[3] we find that the buckling transition in PEA_2MnCl_4 does not induce polarization. For this non-JT-active system, a very different sequence of space groups is observed, despite the fact that the phase transitions occur at comparable temperatures. Inversion symmetry is broken by the rotation of the organic cation, which is independent of the buckling of the inorganic lattice. This leads to a completely different mechanism in which displacements of the organic molecules induce polarization. Notably, we find the resulting polar axis to be out-of-plane. Our results add to the understanding of mechanisms behind ferroelectricity in layered organic-inorganic hybrids.

Single crystals of $(C_6H_5(CH_2)_2NH_3)_2MnCl_4$ were grown by the slow evaporation of the solvent at 60 °C. A 1:2 molar ratio of $MnCl_2$ (Sigma Aldrich; ≥99%) and $C_6H_5(CH_2)_2NH_3Cl$ (2-phenethylamine HCl, Sigma Aldrich; 99%) was dissolved in absolute ethanol (J. T. Baker) and placed in an oven at 60 °C. After approximately one week, *transparent*, *colorless* single crystals had formed. The crystals are shaped as platelets with sizes ranging from 0.1 to around 6 mm.

Single crystal X-ray diffraction (XRD) measurements were performed using a Bruker D8 Venture diffractometer operating with Mo Kα radiation and equipped with a Triumph monochromator and a Photon100 area detector. The crystals were mounted on a 0.5 mm glass fiber using commercial acrylate glue. The crystals were cooled with a nitrogen flow from Oxford Cryosystems Cryostream Plus. Data processing was done using the Bruker Apex III software, the structures were solved using direct methods, and the SHELX97 software[29] was used for structure refinement.

Differential scanning calorimetry (DSC) measurements were performed using TA-instruments STD 2960. An Al crucible was used to measure a powder sample of 38.19 mg over a temperature range of 300 K–450 K at a rate of 1 K/min under a 100 ml/min argon flow.

Differential scanning calorimetry (DSC) measurements reveal two phase transitions, at 363 K and 412 K, as shown in Fig. 1. Furthermore, the onset of weight loss in a corresponding thermogravimetric analysis measurement (not shown) reveals that PEA_2MnCl_4 starts to decompose above 473 K. The phase transition at 363 K is characterized by different slopes before and after the peak; thus, we conclude that it has weak first order character similar to the 340 K transition of the copper analog PEA_2CuCl_4.[3] The second phase transition also appears to be the first order, similar to PEA_2CuCl_4.

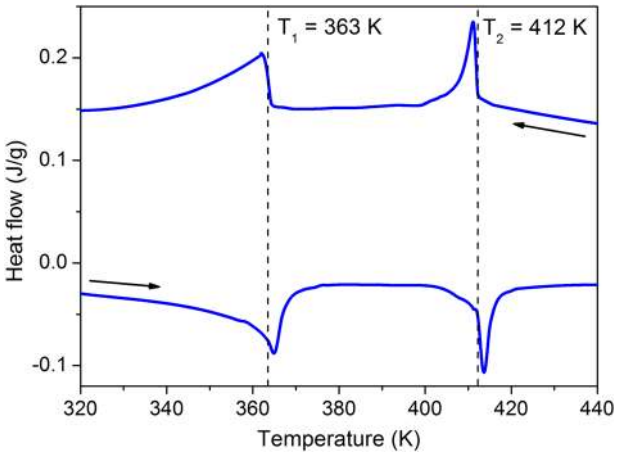

FIG. 1. DSC data showing reversible first-order phase transitions at 363 K and 412 K in PEA_2MnCl_4.

We now focus on the structural investigation of the three different phases indicated by the phase transitions at 363 K and 412 K in Fig. 1. Single-crystal XRD was used to study each crystal structure in detail. Table I summarizes our findings, and the results are discussed below. More extended data, including a list of refined parameters, are shown in Table S1 in the supplementary material. Figure 2 shows the crystal structures of all three phases.

The high-temperature phase is described by the centrosymmetric tetragonal space group *I*4/*mmm*. The reflection conditions clearly indicate either body-centering in the tetragonal setting or face-centering in an orthorhombic setting with a doubled unit cell volume. However, we found that the choice of tetragonal *I*4/*mmm* over orthorhombic *Fmmm* gave significantly better fitting parameters. The individual $MnCl_6$-octahedra have apical Mn-Cl bonds of 2.4633(24) Å and equatorial Mn—Cl bonds of 2.5836(7) Å, respectively. As a consequence of the symmetry, the inorganic layers are perfectly flat, i.e., all Mn—Cl—Mn angles are 180°. Electron density maps suggested that the phenyl rings of the PEA molecules are rotationally disordered around the *c*-axis. The structure as shown in Figs. 2(c) and 3 should thus only be considered as a schematic with respect to the rotational angle of the PEA molecules.

The intermediate-temperature phase is described by the orthorhombic space group *Aea*2. The *a* and *b* unit cell parameters are related to those of the high-temperature phase by a factor of $\sqrt{2}$, whereas the same *c*-axis is retained. As shown in Fig. S1 of the supplementary material, the *A*-centering is apparent from the reflection condition *hkl*: $k + l = 2n$. The reflection condition 0*kl*: $k = 2n$ indicates the presence of a *b*-glide plane perpendicular to the *a*-axis. Furthermore, the reflection condition *h*0*l*: $h = 2n$ indicates the presence of an *a*-glide plane perpendicular to the *b*-axis. Note that the reflection condition for *A*-centering, $k + l = 2n$, automatically implies the conditions *h*0*l*: $l = 2n$, *hk*0: $k = 2n$, 0*k*0: $k = 2n$, and 00*l*: $l = 2n$. The combination of the 0*kl*: $k = 2n$ condition for a *b*-glide plane perpendicular to the *a*-axis with the condition for the *A*-centering, $k + l = 2n$, results in the additional condition of 0*kl*: $l = 2n$. This reflection condition indicates the additional presence of a *c*-glide plane perpendicular to the *a*-axis. Thus, the reflection conditions account for both *b*- and *c*-glide planes perpendicular to the *a*-axis. To avoid confusion in such a situation, De Wolff *et al.*

TABLE I. Crystallographic parameters of the three different phases of PEA_2MnCl_4.

	100(2) K	385(2) K	430(2) K
Space group	$Pca2_1$	*Aea*2	*I*4/*mmm*
Symmetry	Polar	Polar	Centrosymmetric
a (Å)	7.2325(6)	7.2975(6)	5.1672(14)
b (Å)	7.1316(6)	7.2603(6)	5.1672(14)
c (Å)	39.118(4)	39.815(3)	40.046(14)

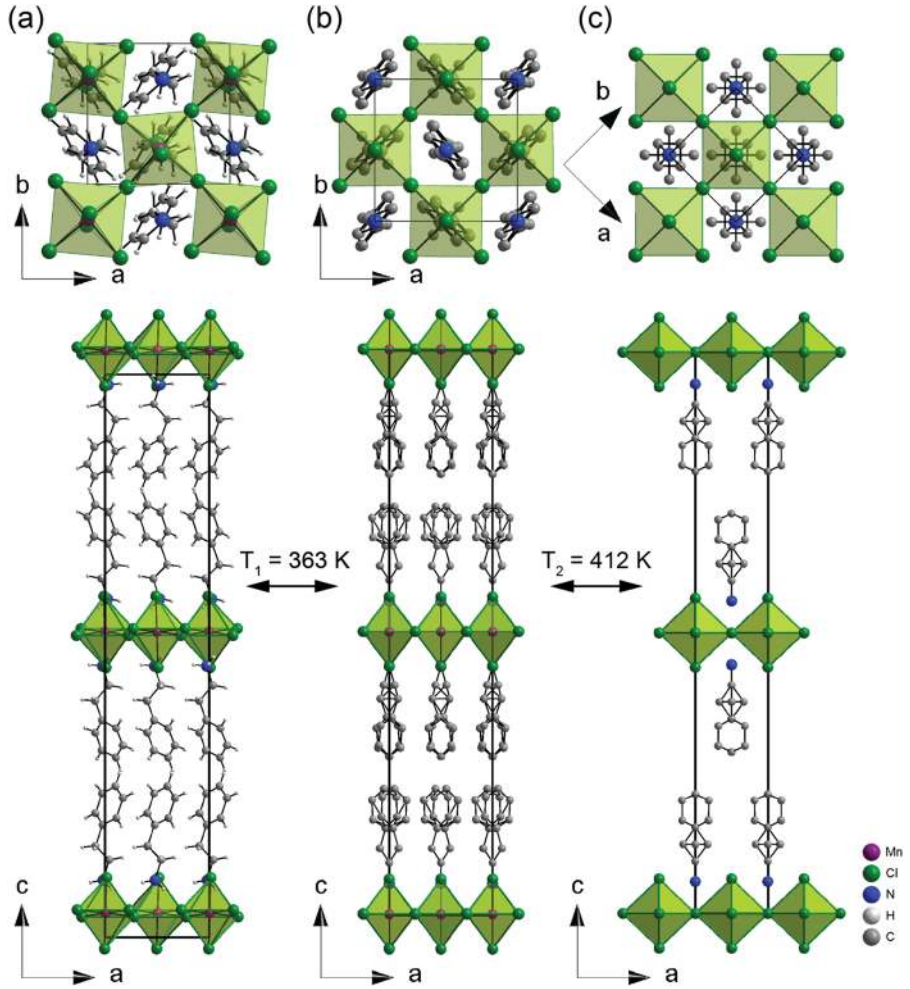

FIG. 2. Crystal structures of the low-temperature $Pca2_1$ (a), intermediate-temperature $Aea2$ (b), and high-temperature $I4/mmm$ (c) phases of $(C_6H_5(CH_2)_2NH_3)_2MnCl_4$. Hydrogen atoms in the intermediate- and high-temperature phase are omitted due to disorder of the organic molecule.

introduced the use of the symbol *e* to cover certain combinations of glide planes that do not have a unique symbol.[30]

The reflection conditions give rise to two possible space groups: the polar *Aea*2 and centrosymmetric *Aeam* (non-standard setting of *Cmce*) space groups, which are both subgroups of the high-temperature *I*4/*mmm* phase.[31] In order to probe centrosymmetry, second harmonic generation (SHG) measurements were performed.[32] SHG is a generally well-suited technique to probe the lack of inversion symmetry in single crystals. Therefore, SHG measurements are often performed to prove the presence of polarization along certain crystal directions. Although SHG measurements were performed on various PEA_2MnCl_4 single crystals, the results were inconclusive. For reference, single crystals of PEA_2CuCl_4 were also probed, which is known to be polar at least up to 340 K.[3] However, SHG measurements on this material were inconclusive as well. It is likely that SHG is not a suitable technique for this specific class of materials, as no conclusions regarding the presence or absence of a polar phase can be made. We reason that this is caused by the very small electrical polarization in our structure. As discussed below in more detail, Mn^{2+} is shifted off-center in the $MnCl_6$-octahedra but only by 1.4 pm. The small associated polarization is most likely impossible to measure with SHG and difficult to detect by any other measurement technique. However, such a displacement is significant compared to the experimental uncertainty of our XRD measurement. Therefore, we continued our analysis using an extensive XRD study.

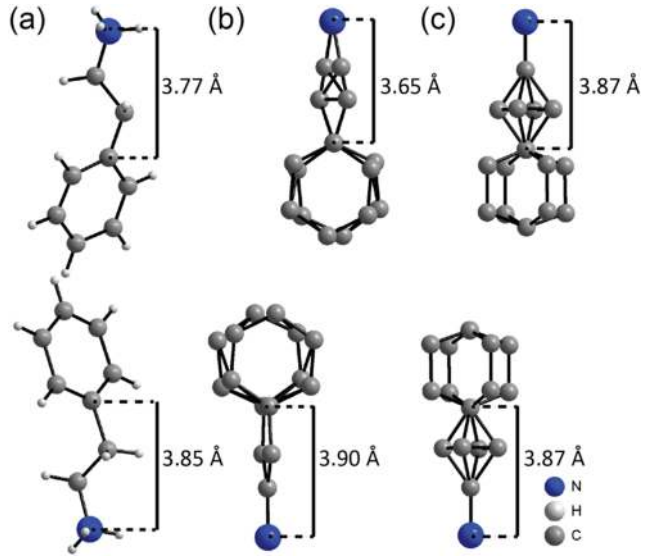

FIG. 3. Ordered and disordered organic cations of the low-temperature $Pca2_1$ (a), intermediate-temperature $Aea2$ (b), and high-temperature $I4/mmm$ (c) phases of $(C_6H_5(CH_2)_2NH_3)_2MnCl_4$. Hydrogen atoms in the intermediate- and high-temperature phase are omitted due to disorder of the organic molecule.

We found $Aea2$ to be the most suitable space group, with inclusion of an inversion twin. Although the structure could be solved and refined in $Aeam$, the polar $Aea2$ space group gave a significantly better fit [$R_1 = 0.0774$ for $Aea2$ and $R_1 = 0.1039$ for $Aeam$, for Fo > 4σ(Fo)]. The intermediate phase appears to be in a pseudodynamic state between the dynamic high-temperature phase with rotating PEA molecules and the frozen low-temperature phase where the PEA molecules have a well-defined orientation (see below). As shown in Fig. 3, the organic cations could be well modeled in the structural refinement by disordering over two positions. This disorder occurs in a kind of tilting manner: the ethylammonium groups are less rigid than the phenyl rings and can be displaced slightly away from the direction perpendicular to the rings. However, this does not occur in exactly the same manner in the two crystallographic distinct organic molecules. Looking at the structure in more detail, it becomes apparent that the organic molecules are responsible for breaking the mirror plane perpendicular to the *c*-axis and hence the inversion symmetry. This occurs by means of a small degree of torsion (with a dihedral angle of around 9.5°) between the two phenyl rings, which are no longer crystallographically equivalent. Therefore, the total structure of the layered hybrid is stacked in an *ABCABC* manner, with *A* and *C* as PEA molecules and *B* as the inorganic layer. By definition, such three-layer structures do not have an inversion center. Therefore, a polar structure is obtained. The fit is poorer in $Aeam$ because the two PEA molecules are related by an additional mirror plane perpendicular to the *c*-axis and hence cannot be rotated with respect to each other. A further consequence of the broken inversion symmetry is that the ethylammonium tails of the two molecules do not approach the space between the $MnCl_6$-octahedra in the inorganic sheets in the same manner. As a result, the tails have significantly different lengths of 3.65 and 3.90 Å, as illustrated in Fig. 3(b). We reason that this difference is caused by different hydrogen bonding patterns. As hydrogen bonding can only occur in a finite number of patterns, it is not possible to optimize the hydrogen bonding of both ammonium groups with chloride simultaneously. Therefore, the ethylammonium tail of one molecule is elongated, allowing the ammonium group to descend further into the void of the inorganic sheet to attain beneficial hydrogen bonding. For the other molecule, the non-optimized hydrogen bonding gives rise to a shorter ethylammonium tail, as unfavorable hydrogen bonding prevents the ammonium group from fully approaching the void between octahedra. As a result, the two positively charged ammonium groups approach the inorganic layer asymmetrically (along the *c*-axis). This also induces the deformation of the negatively charged chlorine cage from a perfect octahedron. Due to this deformation, Mn^{2+} moves off-center along the *c*-axis, contributing to polarization in the structure. The off-center shift of Mn^{2+} is apparent from the difference in apical Mn—Cl bonds: 2.4531(5)

Å and 2.4674(4) Å. Taking the weighted average of the six Cl^- as the center of the octahedron, Mn^{2+} is shifted by around 1.4 pm along the *c*-axis.

In summary, we argue that the out-of-plane polarization is induced by the opening of a small dihedral angle between the planes of the two phenyl groups, which causes an asymmetric approach of the ammonium groups to the inorganic layer, inducing the deformation of the chloride octahedron and a shift of Mn^{2+} off-center along the *c*-axis. The torsion likely originates from competing attractive and repulsive forces in the van der Waals gap between the organic layers. Competing π-π and quadrupole interactions between the phenyl groups can result in the opening of a small dihedral angle between the phenyl ring planes in this pseudodynamic intermediate phase. Notably, vibrational entropy is a factor that can play a dominant role as well.[33] We assign the opening of a small dihedral angle as the primary order parameter for the polar transition. For layered organic-inorganic hybrid structures in general, the organic constituent should have an aromatic group in order to obtain this opening of a dihedral angle between the phenyl ring planes and hence induce out-of-plane polarization. Furthermore, the length of the alkylammonium tail should be sufficient to create asymmetric coupling of the ammonium groups to the inorganic layer and hence deformation of the halide octahedral cage. Shorter tails will limit this degree of freedom and can in fact fix the shape of the entire cation and the way it is incorporated into the crystal structure. Longer alkyl chains may act similarly to PEA. However, this argument may be complicated by the observation that the incorporation of different organic cations can yield very different crystal structures. For example, we have found that exchanging phenethylammonium for 3-phenyl-1-propylamonium in phenethylammonium lead iodide gives rise to a completely different crystal structure with different structural features.[16]

Our finding that the polar axis is out-of-plane is unusual for layered hybrid structures. Buckling of the inorganic layers typically results in a rotational degree of freedom that gives rise to in-plane polarization,[25] as we have previously observed for the copper analog PEA_2CuCl_4,[3] as stated below. Here we show a completely different mechanism, in which displacements of the organic molecules induce an out-of-plane polarization.

The low-temperature phase has previously been reported to exhibit the centrosymmetric orthorhombic *Pbca* space group.[27,28] This space group (in the non-standard setting of *Pcab* in order to keep the labeling of the axes constant for all phases) is consistent with our single-crystal XRD data. All reflection conditions resulting from the three glide planes, i.e., $0kl$: $l = 2n$, $h0l$: $h = 2n$ and $hk0$: $k = 2n$, are obeyed. However, *Pbca* is not a subgroup of the intermediate-temperature phase *Aea*2, as it has higher symmetry.[31] Structure solution and refinement were also successful in the polar space group $Pca2_1$, for which the same reflection conditions apply except for $hk0$: $k = 2n$. Moreover, $Pca2_1$ is a subgroup of *Aea*2.[31] McCabe *et al.* showed in their study on the crystal structure of the Aurivillius phase Bi_2NbO_5F that *Pbca* and $Pca2_1$ can tend to fit equally well and that it can be very difficult to distinguish between the two by single-crystal XRD.[34] Assigning a centrosymmetric space group to a possible polar structure is a common problem in crystallography, especially when the polarization is too small to be measured reliably by other methods. To a first approximation, XRD patterns are always centrosymmetric since the intensities of Friedel Pairs I_{hkl} and I_{-h-k-l} are equal. We have also encountered this dilemma in the copper-based analog, PEA_2CuCl_4. Single-crystal XRD diffraction analysis provided no evidence that the symmetry was lower than centrosymmetric *Pbca* at room temperature,[3] whereas complementary Raman/IR scattering measurements proved the presence of a polar phase.[35] Interpretation of the Raman data suggested that the origin of the polar order lays in a tilt of the organic cation by only ~0.07°, beyond the sensitivity of the XRD measurement. For the low-temperature phase of PEA_2MnCl_4, since any of the three glide planes in the *Pbca* space group can be removed to obtain different settings of $Pca2_1$, we have refined our single-crystal XRD data in not only the centrosymmetric *Pcab* space group but also in all three possible settings of the polar space group: $P2_1ab$, $Pc2_1b$, and $Pca2_1$ (incorporating an inversion twin in each case). Fits using all four structural models are of equal quality, and there is no significant preference for any individual solution based on the data alone. Considering the fact that the polar space group is a direct subgroup of *Aea*2,[31] and that the intermediate phase has an out-of-plane polar axis, we argue that the most likely space group is $Pca2_1$. In this case, the direction of the polar axis is maintained throughout the low- and intermediate-temperature regimes. The low-temperature phase can be considered as a

frozen phase in which the organic cations are ordered, as shown in Figs. 2 and 3. Neighboring phenyl rings are perpendicular to each other, with no significant π-π overlap. Notably, the ethylammonium tails of the two crystallographically independent phenethylammonium molecules differ in length by 8 pm, as shown in Fig. 3(a). This difference is not as large as that for the intermediate phase but still very pronounced. As a result, the low-temperature phase also exhibits a distorted chloride octahedron, where Mn^{2+} is shifted off-center along the *c*-axis. Here, the apical Mn—Cl bonds are 2.4845(3) Å and 2.4973(3) Å, respectively. Taking the weighted average of the six Cl^- as the center of the octahedron, Mn^{2+} is shifted by around 1.1 pm along the *c*-axis, resulting in out-of-plane polarization. However, there is a second possible mechanism that takes place. Both the *Pcab* and $Pca2_1$ space groups allow buckling of the inorganic lattice. We define the buckling angle as the angle between the two apical Cl ions and the *c*-axis. At 100 K, the buckling is around 6.8°. Notably, the choice of space group does not influence the buckling angle: refinement in *Pcab*, $P2_1ab$, $Pc2_1b$, and $Pca2_1$ all resulted in a buckling of 6.8°, within error margins. Figure 4 shows the buckling angle as a function of temperature, measured over all three phases. The buckling is characteristic of the low-temperature phase and disappears above T_1 = 363 K.

The buckling of the inorganic layers appears to be uncoupled from the polar-to-non-polar transition, in contrast to previous work on the copper-based analog PEA_2CuCl_4.[3] In PEA_2CuCl_4, it was found that the polar and buckling transitions appear simultaneously, indicating that the polarization is coupled to the buckling of the inorganic sublattice. Here we show that for PEA_2MnCl_4, the orientational degree of freedom of the organic cation is the driving force for breaking inversion symmetry, independent of the buckling of the inorganic layers.

In conclusion, we have investigated the crystal structures corresponding to three different phases of PEA_2MnCl_4 (PEA = phenethylammonium), using single-crystal XRD analysis, including the group-subgroup analysis of the space groups. Our results show that the high-temperature phase adopts the centrosymmetric *I*4/*mmm* space group, where the organic molecules are fully rotationally disordered. The phase transition at 412 K is governed by a breaking of inversion symmetry and leads to a polar *Aea*2 intermediate-temperature phase. We determined that the low-temperature phase (below 363 K) adopts the space group $Pca2_1$. Notably, the phase transition at 363 K is governed by the onset of the buckling of the inorganic sublattice. In contrast to previous work on the copper-based analog, PEA_2CuCl_4,[3] the buckling transition is not related to the polar-to-non-polar phase transition. In this work, we have thus explored an alternative mechanism that can induce ferroelectricity in organic-inorganic hybrids. In PEA_2MnCl_4, we find that the inversion symmetry is broken by the opening of a small dihedral angle between the two phenyl ring planes of crystallographically inequivalent phenethylammonium molecules. As a result of this dihedral angle, the ethylammonium tails of the two molecules do not approach the space between the $MnCl_6$-octahedra

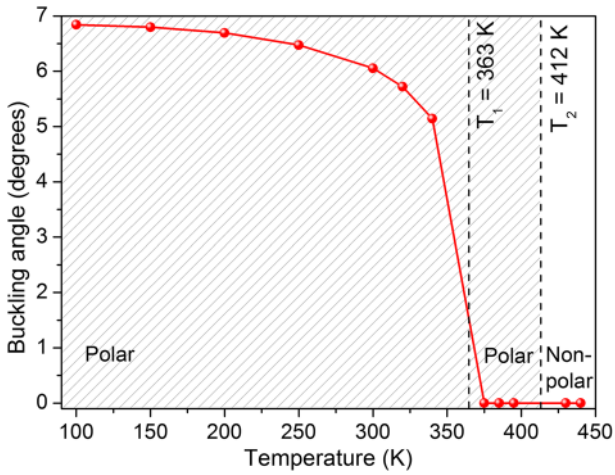

FIG. 4. Buckling angle as a function of temperature in PEA_2MnCl_4. The buckling angle is defined as the angle between the two apical Cl ions and the *c*-axis.

in the inorganic sheets in symmetric fashion. Therefore, a major difference in length between two ethylammonium tails of the two crystallographically independent phenethylammonium groups is observed. We reason that this difference is caused by different hydrogen bonding patterns with the chloride octahedra. Consequently, the negatively charged chlorine cage deforms from perfect octahedral geometry, which results in an off-center shift of Mn^{2+} along the *c*-axis, contributing to the polar nature of the structure. Notably, the polar axis is out-of-plane with respect to the inorganic sheets, in contrast to the in-plane polar axis of similar systems.[3,17] Our findings add to the understanding of possible mechanisms that can induce ferroelectric behavior in layered organic-inorganic hybrids.

See supplementary material for crystallographic data and refinement parameters of the three phases of PEA_2MnCl_4. Crystallographic information files (CIF) are deposited to the CCDC (Cambridge Crystallographic Data Centre) and are available under the following numbers: 1583819 (high-temperature phase, space group *I*4/*mmm*), 1583818 (low-temperature phase, space group $Pca2_1$), and 1583817 (intermediate-temperature phase, space group *Aea*2).

M.E.K. was supported by The Netherlands Organisation for Science NWO (Graduate Programme 2013, No. 022.005.006). R.H. was supported by the ITB Zernike Sandwich Programme. We thank N. Ogawa and Y. Tokura for performing SHG measurements and discussions. We thank A. Caretta and B. Noheda for stimulating discussions.

[1] M. F. Mostafa and R. D. Willett, Phys. Rev. B **4**, 2213 (1971).
[2] W. D. Van Amstel and L. J. De Jongh, Solid State Commun. **11**, 1423 (1972).
[3] A. O. Polyakov, A. H. Arkenbout, J. Baas, G. R. Blake, A. Meetsma, A. Caretta, P. H. M. Van Loosdrecht, and T. T. M. Palstra, Chem. Mater. **24**, 133 (2012).
[4] A. Stroppa, J. Phys.: Conf. Ser. **428**, 12029 (2013).
[5] Z.-K. Tan, R. S. Moghaddam, M. L. Lai, P. Docampo, R. Higler, F. Deschler, M. Price, A. Sadhanala, L. M. Pazos, D. Credgington, F. Hanusch, T. Bein, H. J. Snaith, and R. H. Friend, Nat. Nanotechnol. **9**, 687 (2014).
[6] F. Zhang, H. Zhong, C. Chen, X. Wu, X. Hu, and H. Huang, ACS Nano **9**, 4533 (2015).
[7] G. Xing, N. Mathews, S. S. Lim, N. Yantara, X. Liu, D. Sabba, M. Grätzel, S. Mhaisalkar, and T. C. Sum, Nat. Mater. **13**, 476 (2014).
[8] H. Zhu, Y. Fu, F. Meng, X. Wu, Z. Gong, Q. Ding, M. V. Gustafsson, M. T. Trinh, S. Jin, and X.-Y. Zhu, Nat. Mater. **14**, 636 (2015).
[9] Y. Fang, Q. Dong, Y. Shao, Y. Yuan, and J. Huang, Nat. Photonics **9**, 679 (2015).
[10] Q. Chen, H. Zhou, Z. Hong, S. Luo, H.-S. Duan, H.-H. Wang, Y. Liu, G. Li, and Y. Yang, J. Am. Chem. Soc. **136**, 622 (2014).
[11] D. Liu and T. L. Kelly, Nat. Photonics **8**, 133 (2013).
[12] M. Liu, M. B. Johnston, and H. J. Snaith, Nature **501**, 395 (2013).
[13] W. Ke, G. Fang, J. Wan, H. Tao, Q. Liu, L. Xiong, P. Qin, J. Wang, H. Lei, G. Yang, M. Qin, X. Zhao, and Y. Yan, Nat. Commun. **6**, 6700 (2015).
[14] W. Zhang, M. Saliba, D. T. Moore, S. K. Pathak, M. T. Hörantner, T. Stergiopoulos, S. D. Stranks, G. E. Eperon, J. A. Alexander-Webber, A. Abate, A. Sadhanala, S. Yao, Y. Chen, R. H. Friend, L. A. Estroff, U. Wiesner, and H. J. Snaith, Nat. Commun. **6**, 6142 (2015).
[15] D. B. Mitzi, S. Wang, C. A. Feild, C. A. Chess, A. M. Guloy, and N. Series, Science **267**, 1473 (1995).
[16] M. E. Kamminga, H.-H. Fang, M. R. Filip, F. Giustino, J. Baas, G. R. Blake, M. A. Loi, and T. T. M. Palstra, Chem. Mater. **28**, 4554 (2016).
[17] W.-Q. Liao, Y. Zhang, C.-L. Hu, J.-G. Mao, H.-Y. Ye, P.-F. Li, S. D. Huang, and R.-G. Xiong, Nat. Commun. **6**, 7338 (2015).
[18] Q. Pan, Z.-B. Liu, Y.-Y. Tang, P.-F. Li, R.-W. Ma, R.-Y. Wei, Y. Zhang, Y.-M. You, H.-Y. Ye, and R.-G. Xiong, J. Am. Chem. Soc. **139**, 3954 (2017).
[19] H. Ye, W.-Q. Liao, C.-L. Hu, Y. Zhang, Y.-M. You, J.-G. Mao, P.-F. Li, and R.-G. Xiong, Adv. Mater. **28**, 2579 (2016).
[20] Y.-M. You, W.-Q. Liao, D. Zhao, H.-Y. Ye, Y. Zhang, Q. Zou, X. Niu, J. Wang, P.-F. Li, D.-W. Fu, Z. Wang, S. Gao, K. Yang, J.-M. Liu, J. Li, Y. Yan, and R.-G. Xiong, Science **357**, 306 (2017).
[21] W.-Q. Liao, Y.-Y. Tang, P.-F. Li, Y.-M. You, and R.-G. Xiong, J. Am. Chem. Soc. **139**, 18071 (2017).
[22] J. M. Frost, K. T. Butler, F. Brivio, C. H. Hendon, M. van Schilfgaarde, and A. Walsh, Nano Lett. **14**, 2584 (2014).
[23] S. Liu, F. Zheng, N. Z. Koocher, H. Takenaka, F. Wang, and A. M. Rappe, J. Phys. Chem. Lett. **6**, 693 (2015).
[24] S. Sakai and M. Takahashi, Materials **3**, 4950 (2010).
[25] N. A. Benedek, J. M. Rondinelli, H. Djani, P. Ghosez, and P. Lightfoot, Dalton Trans. **44**, 10543 (2015).
[26] A. O. Polyakov, Ph.D. thesis, University of Groningen, 2014.
[27] S.-H. Park, I.-H. Oh, S. Park, Y. Park, J. H. Kim, and Y.-D. Huh, Dalton Trans. **41**, 1237 (2012).
[28] A. Arkenbout, Ph.D. thesis, University of Groningen, 2010.
[29] G. M. Sheldrick, *SHELX97, Program for Crystal Structure Refinement* (University of Göttingen, Göttingen, 1997).
[30] P. M. De Wolff, Y. Billiet, J. D. H. Donnay, W. Fischer, R. B. Galiulin, A. M. Glazer, T. Hahn, M. Senechal, D. P. Shoemaker, H. Wondratschek, A. J. C. Wilson, and S. C. Abrahams, Acta Crystallogr., Sect. A: Found. Crystallogr. **48**, 727 (1992).
[31] S. Ivantchev, E. Kroumova, G. Madariaga, J. M. Pe, and M. I. Aroyo, J. Appl. Crystallogr. **33**, 1190 (2000).

[32] After SHG measurements by and discussion with N. Ogawa and Y. Tokura, RIKEN Center for Emergent Matter Science (CEMS), Hirosawa, Japan.
[33] K. T. Butler, K. Svane, G. Kieslich, A. K. Cheetham, and A. Walsh, Phys. Rev. B **94**, 180103 (2016).
[34] E. E. McCabe, I. P. Jones, D. Zhang, N. C. Hyatt, and C. Greaves, J. Mater. Chem. **17**, 1193 (2007).
[35] A. Caretta, R. Miranti, R. W. A. Havenith, E. Rampi, M. C. Donker, G. R. Blake, M. Montagnese, A. O. Polyakov, R. Broer, T. T. M. Palstra, and P. H. M. van Loosdrecht, Phys. Rev. B **89**, 24301 (2014).